# Layer-Based Integration Arithmetic of Conformal PML

**Y. J. Zhang and Q. Sun**

School of Aeronautics
Northwestern Polytechnical University, Xi'an, 710072, P.R. China
zyj19191@nwpu.edu.cn

***Abstract*** **–** As an efficient artificial truncating boundary condition, conformal perfectly matched layer (CPML) is a multilayer anisotropic absorbing media domain. The conventional finite element analysis of CPML generates a large scale coefficient matrix that leads to prohibitive cost to solve. This paper proposes layer-based integration arithmetic, in which, the CPML multilayer integration is substituted by layer-wise summing of monolayer integration on the normal direction, with considering relative dielectric constant and permeability as constants in each very thin monolayer. The arithmetic needs to divide CPML into through-thickness elements of multiple layers, while the coefficient matrix of each element is evaluated by the layer-based integration. Numerical experiments show that the layer-based integration arithmetic is reliable and CPML under this arithmetic becomes a high-efficiency absorbing boundary condition.

***Keywords:*** conformal PML, layer-based integration arithmetic, and absorbing boundary condition.

## NOMENCLATURE

| | |
|---|---|
| $\mu_r$ | relative permeability |
| $\varepsilon_r$ | relative dielectric constant |
| $k_0$ | wave number |
| $\lambda$ | wave length |
| $\boldsymbol{E}$ | electric field |
| $\overline{\overline{\Lambda}}$ | constitutive parameter of PML in tensor |
| $\lvert\boldsymbol{A}\rvert$ | determinant of matrix $\boldsymbol{A}$ |
| $\boldsymbol{A}^{-1}$ | inverse matrix of matrix $\boldsymbol{A}$ |
| time | time of iterations, unit is second |

## I. INTRODUCTION

The perfectly matched layer (PML) concept introduced by Berenger [l], is an efficient method for truncating the unbounded spatial domain in electromagnetic radiation and scattering problems. Although the PML approach was originally introduced in the context of the finite-difference time-domain (FDTD) method [l], it has been found useful [2] in mesh truncation in the finite element method (FEM) as well. It has recently been verified that artificial anisotropic media, with properly designed permittivity and permeability tensors, can absorb electromagnetic waves irrespective of their frequency and angle of incidence [3]. Kuzuoglu and Mittra [4] designed first conformal PML, which provides an efficient FEM mesh truncation, especially for problems involving electrically large antennas and complicated scatterers. Some versions of the conformal PML (CPML) suited to the FEM implementation were generalized in [5, 6].

For problems as demanding of computational resources as electromagnetic scattering, the conformal PML boundary is always desirable. Generally 6~10 layers of conformal PML meet absorbing condition, but more layers are needed for large complicated scatterers. Unfortunately, the layer is so thin that CPML is divided into large quantity of elements in adequate fine size, and finite element analysis of CPML generates a large scale coefficient matrix that leads to prohibitive cost to solve. For reducing quantity of elements, some research works [7-10] are implemented, but not settle this problem completely. To overcome this difficulty, we develop layer-based integration arithmetic, in which, multilayer integration of CPML elements is substituted by layer-wise summing of monolayer integration on the normal direction.

The contents of this paper include the layer-based integration arithmetic of conformal PML, arithmetic implementation and numerical experiments, which demonstrate both the applicability and effectiveness of the arithmetic.

## II. CONFORMAL PML FORMULATION

In this section, we start by reviewing the definition of the conformal PML [5]; only the equations relevant to our implementation are presented.

For a general anisotropic PML, the constitutive parameters must be of the form $\overline{\overline{\mu}} = \mu_r \overline{\overline{\Lambda}}$ and $\overline{\overline{\varepsilon}} = \varepsilon_r \overline{\overline{\Lambda}}$. In the case of a conformal PML, the tensor is expressed as,

$$\overline{\overline{\Lambda}} = \boldsymbol{uu}\left(\frac{s_2 s_3}{s_1}\right) + \boldsymbol{vv}\left(\frac{s_1 s_3}{s_2}\right) + \boldsymbol{ww}\left(\frac{s_1 s_2}{s_3}\right). \tag{1}$$

Here, the conformal PML domain is a smooth convex shell, which encloses the scatterer a small distance away. Let $\boldsymbol{S}$ be the inner surface of this shell; at any given point $\boldsymbol{P}$ on $\boldsymbol{S}$, the unit vectors $\boldsymbol{u}$ and $\boldsymbol{v}$ coincide with the principal directions, and $\boldsymbol{w}$ is the unit surface normal. Assume that there are local coordinates $u$, $v$ and $w$ running in the $\boldsymbol{u}$, $\boldsymbol{v}$, and $\boldsymbol{w}$ directions, and $w$ takes the value zero on surface $\boldsymbol{S}$; then the points of constant $w$ correspond to a parallel surface $\boldsymbol{S}'$ at a distance $w$ from $\boldsymbol{S}$. If the principal radii at point $\boldsymbol{P}$ are given by $r_{01}(u,v)$ and $r_{02}(u,v)$, then for point $\boldsymbol{P}'(u,v,w)$ on $\boldsymbol{S}'$, they will be given by $r_1(u,v,w)=r_{01}(u,v)+w$ and $r_2(u,v,w)=r_{02}(u,v)+w$.

The tensor values in the parentheses give geometrical and physical information on the conformal PML as,

$$\begin{cases} s_1 = \left(r_{01} + \int_0^w s(\zeta)d\zeta\right) \Big/ r_1 \\ s_2 = \left(r_{02} + \int_0^w s(\zeta)d\zeta\right) \Big/ r_2 \\ s_3 = s \end{cases} \tag{2}$$

where $s$ is the complex stretching variable [5] in the $w$-direction.

Assume that $u$, $v$, $w$ are coordinate component in local coordinate system $\boldsymbol{u}$, $\boldsymbol{v}$, and $\boldsymbol{w}$, so matrix of $\overline{\overline{\Lambda}}$ in local coordinate system is given by,

$$\overline{\overline{\Lambda}}_{u.v,w} = \begin{bmatrix} \frac{s_2 s_3}{s_1} & 0 & 0 \\ 0 & \frac{s_1 s_3}{s_2} & 0 \\ 0 & 0 & \frac{s_1 s_2}{s_3} \end{bmatrix}. \tag{3}$$

## III. LAYER-BASED INTEGRATION ARITHMETIC

For 3-D electromagnetic scattering solution under PML absorbing boundary, scattering field can be described as following vector wave equations,

$$\nabla \times \left( \frac{1}{\mu_r} \overline{\overline{\Lambda}}^{-1} \cdot \nabla \times \boldsymbol{E}^s \right) - k_0^2 \varepsilon_r \overline{\overline{\Lambda}} \cdot \boldsymbol{E}^s = \boldsymbol{0} \tag{4}$$

where $\boldsymbol{E}^s$ is scattering electric field.

Applying variational principle to equation (4), the resulting functional is written as,

$$F\left(\boldsymbol{E}^s\right) = \frac{1}{2} \iiint_V \left[ \frac{1}{\mu_r} \left(\nabla \times \boldsymbol{E}^s\right) \cdot \overline{\overline{\Lambda}}^{-1} \cdot \left(\nabla \times \boldsymbol{E}^s\right) - k_0^2 \varepsilon_r \boldsymbol{E}^s \cdot \overline{\overline{\Lambda}} \cdot \boldsymbol{E}^s \right] dV. \tag{5}$$

The functional (5) is discretized by finite elements; formulation of element matrix is expressed as,

$$K_{ij} = \iiint_V \frac{1}{\mu_r} \left(\nabla \times \boldsymbol{N}_i\right) \cdot (\overline{\overline{\Lambda}})^{-1} \cdot \left(\nabla \times \boldsymbol{N}_j\right) dV - \iiint_V k_0^2 \varepsilon_r \boldsymbol{N}_i \cdot \overline{\overline{\Lambda}} \cdot \boldsymbol{N}_j dV \tag{6}$$

where $\boldsymbol{N}_i$ and $\boldsymbol{N}_j$ are vector basis functions.

The conformal PML is multilayer anisotropic absorbing media that is shown as Fig. 1, so formulation of the $k^{\text{th}}$ layer element matrix is written as,

$$K_{ij\_k} = \iiint_V \left(\nabla \times \boldsymbol{N}_i\right) \cdot (\overline{\overline{\mu}}_{rk})^{-1} \cdot \left(\nabla \times \boldsymbol{N}_j\right) dV - \iiint_V k_0^2 \boldsymbol{N}_i \cdot \overline{\overline{\varepsilon}}_{rk} \cdot \boldsymbol{N}_j dV \tag{7}$$

where $k$ is number of medium layer, $n$ is total layer number, $h_k$ is thickness of the $k^{\text{th}}$ layer, $\overline{\overline{\mu}}_{rk} = \mu_r \overline{\overline{\Lambda}}_k$ and $\overline{\overline{\varepsilon}}_{rk} = \varepsilon_r \overline{\overline{\Lambda}}_k$ are relative dielectric constant and permeability of the $k^{\text{th}}$ layer conformal PML, $\overline{\overline{\Lambda}}_k$ is determined by geometric parameters of the $k^{\text{th}}$ layer.

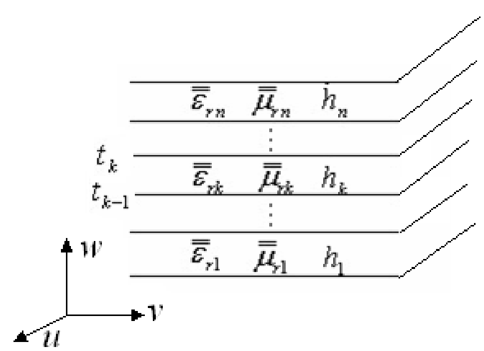


Fig. 1. n layers of conformal PML.

Because monolayer of conformal PML is very thin, layer-face size of solid element should be enough fine to match the thin thickness of monolayer. Especially, when CPML possesses many layers, CPML domain is divided into large quantities of solid elements. The conventional finite element analysis of CPML generates a large scale coefficient matrix that leads to prohibitive cost to solve.

Fortunately, relative dielectric constant and permeability may be considered as constants in each thin layer, so CPML multilayer integration is substituted by layer-wise summing of monolayer integration on the normal direction. The arithmetic needs to divide CPML into through-thickness elements of multiple layers, while the coefficient matrix of each element is evaluated by the layer-based integration. Detail is described as following.

Right hand of equation (6) is rewritten as two integrals,

$$A_{ij} = \iiint_V \frac{1}{\mu_r}\left(\nabla \times \boldsymbol{N}_i\right)\cdot(\overline{\overline{\Lambda}})^{-1}\cdot\left(\nabla \times \boldsymbol{N}_j\right)dV \tag{8}$$

$$B_{ij} = \iiint_V k_0^2 \varepsilon_r \boldsymbol{N}_i \cdot \overline{\overline{\Lambda}} \cdot \boldsymbol{N}_j dV \ . \tag{9}$$

In equation (8) layer-based integration along the normal direction is written as,

$$\begin{aligned} A_{ij} &= \iiint_V \frac{1}{\mu_r}\left(\nabla \times \mathbf{N}_i\right)\cdot(\overline{\overline{\Lambda}})^{-1}\cdot\left(\nabla \times \mathbf{N}_j\right)dV \\ &= \int_{-1}^{1}\int_{-1}^{1}\int_{-1}^{1}\frac{1}{\mu_r}\left(\nabla \times \mathbf{N}_i\right)\cdot(\overline{\overline{\Lambda}})^{-1} \\ &\quad \cdot\left(\nabla \times \mathbf{N}_j\right)\cdot|J|dudvdw \\ &= \int_{-1}^{1}\int_{-1}^{1}\left[\sum_{k=1}^{n}\int_{t_{k-1}}^{t_k}\left(\nabla \times \mathbf{N}_i\right)\cdot(\overline{\overline{\mu}}_{rk})^{-1}\right. \\ &\quad \left.\cdot\left(\nabla \times \mathbf{N}_j\right)\cdot|J|dw\right]dudv \\ &= \int_{-1}^{1}\int_{-1}^{1}\left[\sum_{k=1}^{n}\int_{-1}^{1}\left(\nabla \times \mathbf{N}_i\right)\cdot(\overline{\overline{\mu}}_{rk})^{-1}\right. \\ &\quad \left.\cdot\left(\nabla \times \mathbf{N}_j\right)\cdot|J|\frac{h_k}{t}dw_k\right]dudv \end{aligned} \tag{10}$$

where $J$ is 3-D isoparametric Jacobi matrix [11], $t$ is total thickness of conformal PML.

$$J = \begin{bmatrix} \frac{\partial x}{\partial u} & \frac{\partial y}{\partial u} & \frac{\partial z}{\partial u} \\ \frac{\partial x}{\partial v} & \frac{\partial y}{\partial v} & \frac{\partial y}{\partial v} \\ \frac{\partial x}{\partial w} & \frac{\partial z}{\partial w} & \frac{\partial z}{\partial w} \end{bmatrix} \tag{11}$$

$$t = \sum_{m=1}^{n} h_m \ , \tag{12}$$

$$t_k = t_{k-1} + \frac{2h_k}{t}, \quad k = 1,2,\cdots n, \qquad t_0 = -1, \tag{13}$$

$$\begin{aligned} w &= \frac{1-w_k}{2}t_{k-1} + \frac{1+w_k}{2}t_k \\ &= \frac{1-w_k}{2}\left(t_k - \frac{2h_k}{t}\right) + \frac{1+w_k}{2}t_k \\ &= \frac{h_k}{t}\left(w_k - 1\right) + t_k \end{aligned} \tag{14}$$

where $h_k$ is small enough, so we simplify integration function in equation (10) as,

$$\begin{aligned} A_{ij} = \int_{-1}^{1}\int_{-1}^{1}&\left[\sum_{k=1}^{n}\left(\nabla \times \boldsymbol{N}_i\right)\cdot(\overline{\overline{\mu}}_{rk})^{-1}\right. \\ &\left.\cdot\left(\nabla \times \boldsymbol{N}_j\right)A_k h_k\right]dudv \end{aligned} \tag{15}$$

where $A_k$ is integrating factor of $|J|$ on the surface $w_k = 0$,

$$\begin{cases} A_k = \sqrt{A_{kx}^2 + A_{ky}^2 + A_{kz}^2}\,|_k \\ A_{kx} = \frac{\partial y}{\partial u}\frac{\partial z}{\partial v} - \frac{\partial z}{\partial u}\frac{\partial y}{\partial v} \\ A_{ky} = \frac{\partial z}{\partial u}\frac{\partial x}{\partial v} - \frac{\partial x}{\partial u}\frac{\partial z}{\partial v} \\ A_{kz} = \frac{\partial x}{\partial u}\frac{\partial y}{\partial v} - \frac{\partial y}{\partial u}\frac{\partial x}{\partial v} \end{cases} . \tag{16}$$

Similarly, layer-based integration formula of equation (9) can be obtained,

$$B_{ij} = \int_{-1}^{1}\int_{-1}^{1}\left[\sum_{k=1}^{n} k_0^2 \boldsymbol{N}_i \cdot \overline{\overline{\varepsilon}}_{rk} \cdot \boldsymbol{N}_j A_k h_k\right]dudv \, . \tag{17}$$

Considering that electromagnetic field distribution is nonlinear in multilayer of conformal PML, second-order or higher order vector basis functions are essential to evaluation precision in the layer-based integration arithmetic. In this paper, we employ second-order vector basis functions [12].

## IV. NUMERICAL EXPERIMENTS

In this section, in order to verify the accuracy and efficiency of layer-based integration arithmetic, we implement the arithmetic in three classical experiments.

1- Metal sphere, its diameter is $0.666\lambda$ , incidence wave spreads along $z$ , frequency is 300 MHz, as following Fig. 2(a).

2- Metal ellipsoid shell, its major axis is $1.0\lambda$, its minor axis is $0.5\lambda$, incidence wave spreads along $Z$, frequency is 3 GHz, as following Fig. 2(b).

3- Metal wing, its span length is $5.0\lambda$, its chord length is $2.46\lambda$, its maximum height is $0.28\lambda$, incidence wave spreads along $X$, frequency is 300 MHz, as following Fig. 2(c).

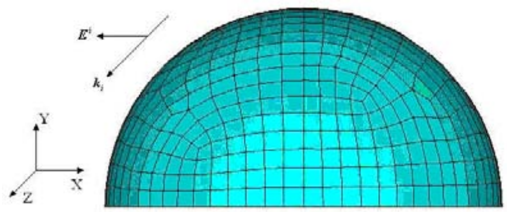


Fig. 2(a). Metal sphere.

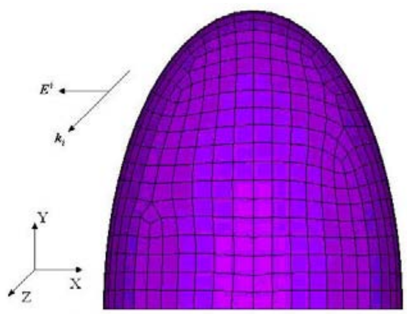


Fig. 2(b). Metal ellipsoid shell.

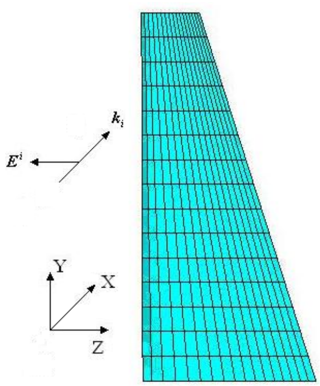


Fig. 2(c). Metal wing.

In the experiments, we employ curve hexahedra vector element in [12] and ICCG method to solve system equations in [13]. Results are obtained with 512M-memory computer. All programs are developed in FORTRAN90 compiled language.

In Fig. 3, we compare evaluation precision of the layer-based integration arithmetic with 6 layers of CPML for solving bistatic RCS of experiments under different element sizes. $\theta$ and $\varphi$ are spherical coordinates. The results show that CPML under the layer-based integration arithmetic is more accurate and reasonable under $\lambda/50$ element size. The main cause is that the normal direction and principal radius of curvature of CPML are calculated more accurately under $\lambda/50$ element size than under $\lambda/20$ element size, especially on small curvature radius domain.

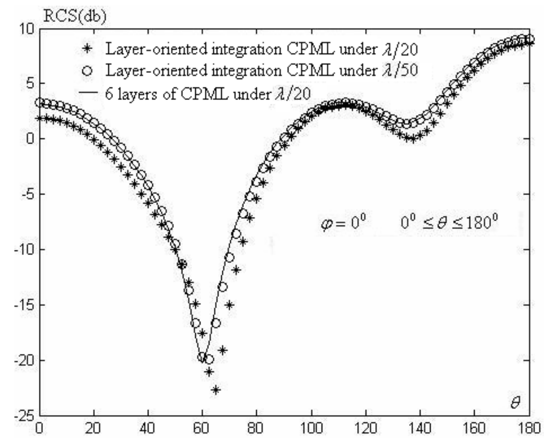


Fig. 3(a). Bistatic RCS of metal sphere.

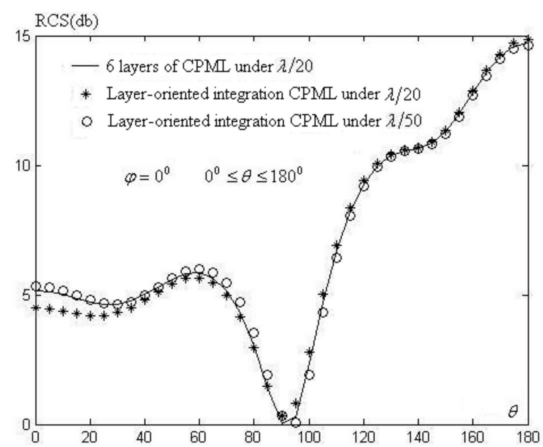


Fig. 3(b). Bistatic RCS of metal ellipsoid shell.

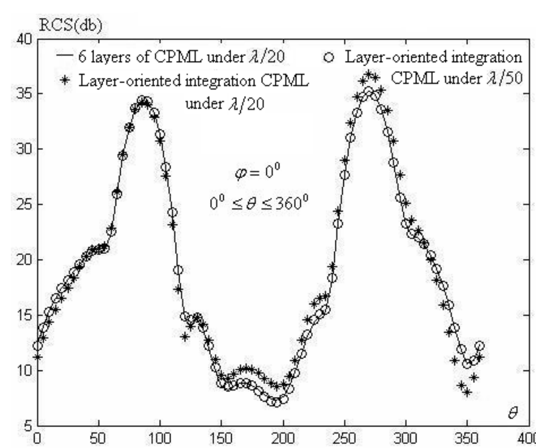


Fig. 3(c). Forward bistatic RCS of metal wing.

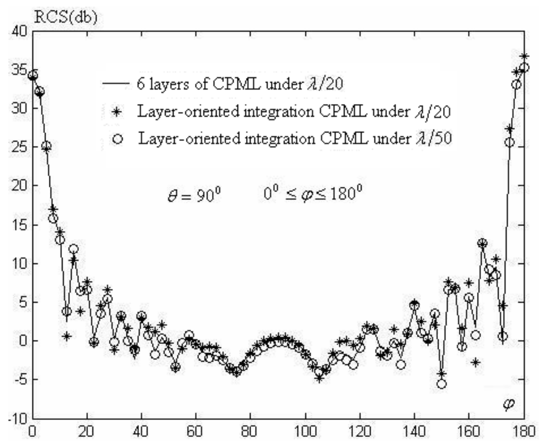

Fig. 3(d). Side bistatic RCS of metal wing.

In Table 1, we compare scale and speed of the layer-based integration arithmetic with 6 layers of CPML under different element sizes. The results show that CPML under the layer-based integration arithmetic costs much less scale and time than 6 layers of CPML.

Table 1. Scale and time of solution

| Ex | CPML | Element size | Element quantity | Time(s) |
|---|---|---|---|---|
| 1 | 6 layers | $\lambda/20$ | 14880 | 16.97 |
|  | layer-based integration | $\lambda/50$ | 8542 | 9.124 |
| 2 | 6 layers | $\lambda/20$ | 83455 | 112.5 |
|  | layer-based integration | $\lambda/50$ | 51668 | 70.36 |
| 3 | 6 layers | $\lambda/20$ | 180112 | 264.3 |
|  | layer-based integration | $\lambda/50$ | 117466 | 149.2 |

## V. CONCLUSION

For reducing quantity of elements in multilayer CPML domain, we develop the layer-based integration arithmetic to evaluate integrations of multilayer elements. In view of its high efficiency on complicated objects, CPML under this arithmetic shows great promise as an ideal absorber for electromagnetic scattering analysis.

## ACKNOWLEDGEMENT

The support of Science and technology Innovation Foundation of Northwestern Polytechnical University (W016143) is gratefully acknowledged.

The support of National Natural Science Foundation of China (No. 10477018) is gratefully acknowledged.

## REFERENCES

[1] J. P. Berenger, "A perfectly matched layer for the absorption of electromagnetic waves," *L Comp. Phys.*, vol. 114, no. 2, pp. 185-200, 1994.

[2] U. Peke1 and R. Mittra, "A finite element method frequency-domain application of the perfectly matched layer (PML) concept," *Microwave Opt. Technol. Lett.*, vol. 9, no. 8, pp. 117-122, 1995.

[3] Z. S. Sacks, D. M. Kingsland, R. Lee, and J.-F. Lee, "A perfectly matched anisotropic absorber for use as an absorbing boundary condition," *IEEE Trans. Antennas Propagat.,* vol. 43, no. 12, pp. 1460-1463, 1995.

[4] M. Kuzuoglu and R. Mittra, "Mesh truncation by perfectly matched anisotropic absorbers in the finite element method," *Microwave Opt. Technol. Lett.*, vol. 12, no. 3, pp. 136-140, 1996.

[5] F. L. Teixeira and W. C. Chew, "Analytical derivation of a conformal perfectly matched absorber for electromagnetic waves," *Microwave Opt. Technol. Lett*., vol. 17, no. 4, pp. 231-236, 1998.

[6] P. Liu, J. D. Xu, and W. Wan, "A finite-element realization of a 3-d conformal pml*," Microwave Opt. Technol. Lett*., vol. 30, no. 3, pp. 170-173, 2001.

[7] C. Guérin and G. Tanneau, "A shell element for computing 3D eddy currents -application to transformers*," IEEE Trans. Magn.*, vol. 31, no. 3, pp. 1360–1363, 1995.

[8] J. M. Jin, *The Finite Element Method in Electromagnetics*, 2nd ed., New York: Wiley, 2002.

[9] A. L. Radovinskii, "General theorems of the electromechanics of thin elastic shells," *Journal of Applied Mathematics and Mechanics*, vol. 53, no. 4, pp. 514–519, 1989.

[10] Rajeev Thottappillil, Martin A. Uman, and Nelson Theethayi, "Electric and magnetic fields from a semi-infinite antenna above a conducting plane," *Journal of Electrostatics*, vol. 61, no. 3, pp. 209–221, 2004.

[11] Weng Cho Chew, *Fast and Efficient Algorithms in Computational Electromagnetics*, Boston: Artech House, 2001.

[12] Li jianghai and Sun qin, "Constructing a class of orthogonal-reinforced hierarchical hexahedra vector FE," *Chinese Journal for Computational Physics*, vol. 23, no. 1, pp. 32-36, 2006.

[13] Y. J. Zhang and Q. Sun, "Improved ICCG method for large scale sparse linear equations," *Chinese Journal of Computational Physics*, vol. 24, no. 5, pp. 581-584, 2007.